catalysts

MDPI

Article

Palladium-Catalyzed Domino Cycloisomerization/Double Condensation of Acetylenic Acids with Dinucleophiles

Nerea Conde, María Teresa Herrero, Garazi Urgoitia and Raul SanMartin *

Department of Organic and Inorganic Chemistry, Faculty of Science and Technology, University of the Basque Country (UPV/EHU), 48940 Leioa, Spain; nerea.conde@ehu.eus (N.C.); mariateresa.herrero@ehu.eus (M.T.H.); garazi.urgoitia@ehu.eus (G.U.)

* Correspondence: raul.sanmartin@ehu.eus

Abstract: Metal-catalyzed cascade processes based on hydrofunctionalization of alkynes are receiving much more attention because of their potential to provide advantageous approaches to otherwise synthetically challenging compounds. An alternative catalyst system has been found for the domino cycloisomerization/cyclocondensation reaction involving acetylenic acids and heterodinucleophiles. A CNN pincer palladium(II) complex, acting as a homogeneous catalyst, provides the corresponding polyheterocycles with a higher substrate/catalyst ratio. Other palladium sources were also tested and discarded, and a number of mechanistic studies including poisoning assays, kinetic plots, TEM images, XRD spectra and UPLC-MS analysis of reaction intermediates were conducted in order to shed light on the role of this pincer catalyst and the catalytic cycle involved in the cascade reaction. As a result, a more nuanced mechanism is tentatively proposed.

Keywords: palladium; domino reactions; alkynes

Citation: Conde, N.; Herrero, M.T.; Urgoitia, G.; SanMartin, R. Palladium-Catalyzed Domino Cycloisomerization/Double Condensation of Acetylenic Acids with Dinucleophiles. *Catalysts* **2022**, *12*, 127. https://doi.org/10.3390/catal12020127

Academic Editors: Thomas J. J. Müller and Eelco Ruijter

Received: 18 December 2021
Accepted: 17 January 2022
Published: 21 January 2022

Publisher's Note: MDPI stays neutral with regard to jurisdictional claims in published maps and institutional affiliations.

1. Introduction

Metal-catalyzed cascade reactions have attracted much more attention as an expeditious access to relatively complex frameworks from readily available substrates. In this regard, the construction of cyclic or polycyclic structures by means of cascade processes involving alkynes is a rapidly emerging field on account of the increasing number of reports on this topic [1–4]. A particularly appealing cascade reaction between alkynoic acids and dinucleophiles was discovered due to the elegant works by Dixon [5–7], Patil [8,9], Liu-Zhao [10–17], Reddy [18,19] and Lei [20]. Au(I) (often Au(I)-Ag(I)), Cu(II), and recently, Ru(II) catalysts were the key for this transformation leading to a number of polyheterocycles, including structural analogues of quinazoline alkaloids *Tryptanthrine*, *Batracyclin*, *Peganine*, *Vasicinone*, or *Mackinazoline*, and the inhibitor of aldo-keto reductase AKR1C3 depicted in Figure 1 [21,22]. In most cases, a plausible reaction mechanism has been proposed, suggesting an initial cycloisomerization of the alkynoic acid followed by a nucleophilic attack at the corresponding enol lactone intermediate to form a ketonamide that under acidic (Brönsted or Lewis) conditions leads to the cyclized product via an acyliminium ion intermediate (Scheme 1). A minimum amount of 0.5 mol% of metal catalyst is required to affect the cascade process (catalyst loading ranging from 0.5 to 20 mol%) [5–19].

Following our research on metal-catalyzed transformations involving alkynes [23], we had described an unprecedented amount of activity for the cycloisomerization of alkynoic acids exhibited by a palladium NNC complex (**1**) [24]. On this basis, we envisaged that such a more active catalyst could also promote a domino process leading to polyheterocyclic structures if reacted with suitable dinucleophiles. In addition to a new metal participating in this reaction, this approach could lead to a substantial enhancement in the catalytic efficiency, which is increasingly becoming a priority in sustainable chemistry [25–27]. In this regard, we wish to present an exceedingly active catalyst system for the cascade

reaction between alkynoic acids and *N*,*O*- and *N*,*N*-dinucleophiles as well as an insight into the reaction mechanism.

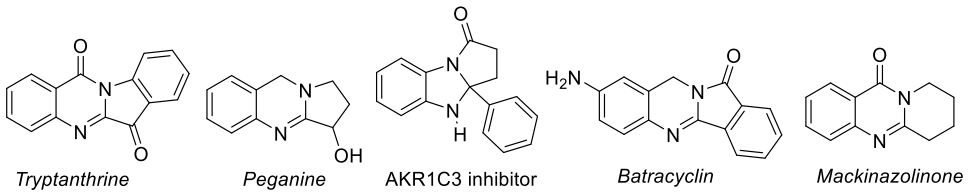

Figure 1. Structure of quinazoline alkaloids and reductase inhibitor pyrrolobenzimidazolone.

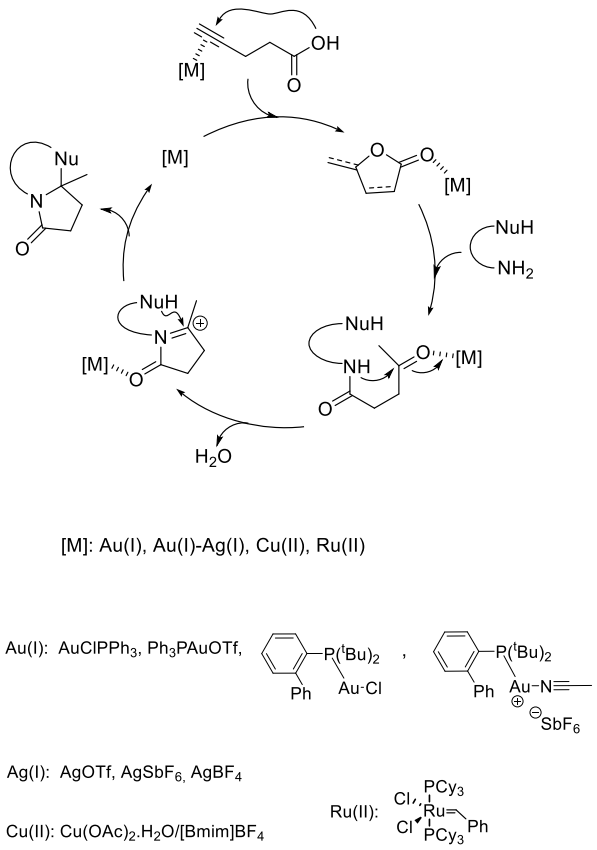

Scheme 1. Postulated catalytic cycle and reported metal catalysts for the cascade reaction between alkynoic acids and dinucleophiles.

2. Results and Discussion

Pentynoic acid **2a** and anthranilic acid **3a** were chosen as model substrates for a number of initial assays. Different palladium sources ($Pd(OAc)_2$, $PdCl_2$, and $Pd(PPh_3)_4$) were tested, and the results compared to those obtained from NNC palladium complex **1**. The catalyst loading was set at 10^{-2} mol% in order to meet the aforementioned requirements of efficiency. The amounts of base and/or additive were also minimized following the same criteria. After a number of initial experiments, it became clear that the process required chloroform as a solvent and triethylamine as a base to get reasonable yields, as negligible results were obtained from other bases (KOH, NaOH, LiOH, KO^tBu, K_2CO_3, Cs_2CO_3, DBU, DIPEA, pyridine and DMAP) and solvents (THF, PhMe, MeOH, CH_2Cl_2, DMF, DMA, DMSO and MeCN) (see Supplementary Material for further details).

Only pincer complex **1** provided target benzopyrrolo[1,3]oxazine-1,5-dione **4a** even using triethylamine in chloroform (Figure 2, entries 1–4), and the presence of a Lewis acid additive proved beneficial for the reaction outcome (entries 5–9).

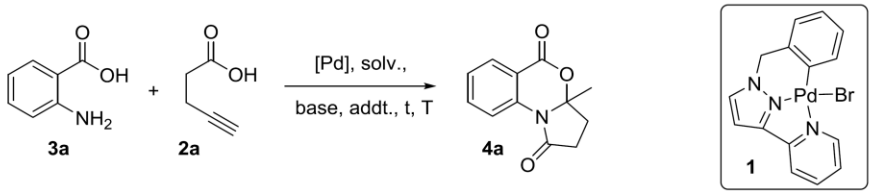

Entry	solv. (M)	[Pd] (mol%)	Base	Additive	T (°C)	t (h)	4a (%) [b]
1	$CHCl_3$ (0.1)	**1** (10^{-2})	Et_3N	-	60	96	14
2	$CHCl_3$ (0.1)	$Pd(OAc)_2$ (10^{-2})	Et_3N	-	60	96	-
3	$CHCl_3$ (0.1)	$Pd(OAc)_2$ (10^{-2})	Et_3N	-	120	96	-
4	$CHCl_3$ (0.1)	$PdCl_2$ (10^{-2})	Et_3N	-	60	96	-
5	$CHCl_3$ (0.1)	**1** (10^{-2})	Et_3N	*p*-TsOH	60	96	15
6	$CHCl_3$ (0.1)	**1** (10^{-2})	Et_3N	$BF_3{\cdot}O(C_2H_5)_2$	60	96	20
7	$CHCl_3$ (0.1)	**1** (10^{-2})	Et_3N	$AlCl_3$	60	96	27
8	$CHCl_3$ (0.1)	**1** (10^{-2})	Et_3N	$FeCl_3$	60	96	45
9	$CHCl_3$ (0.1)	**1** (10^{-2})	Et_3N	$FeBr_2$	60	96	48
10	$CHCl_3$ (0.1)	**1** (10^{-2})	Et_3N	$FeBr_2$	120	96	79
11	$CHCl_3$ (0.1)	**1** (10^{-4})	Et_3N	$FeBr_2$	120	96	39
12 [c]	$CHCl_3$ (0.1)	**1** (10^{-2})	Et_3N	$FeBr_2$	120	96	24
13 [d]	$CHCl_3$ (0.1)	**1** (10^{-2})	Et_3N	$FeBr_2$	120	96	69
14 [e]	$CHCl_3$ (0.1)	**1** (10^{-2})	Et_3N	$FeBr_2$	120	96	85
15 [e]	$CHCl_3$ (0.2)	**1** (10^{-2})	Et_3N	$FeBr_2$	120	96	85
16 [e]	$CHCl_3$ (0.02)	**1** (10^{-2})	Et_3N	$FeBr_2$	120	96	<5
17 [e]	$CHCl_3$ (0.5)	**1** (10^{-2})	Et_3N	$FeBr_2$	120	96	93
18 [e]	$CHCl_3$ (1)	**1** (10^{-2})	Et_3N	$FeBr_2$	120	96	59
19 [e]	$CHCl_3$ (0.5)	**1** (10^{-2})	Et_3N	$FeBr_2$	120	72	71
20 [e]	$CHCl_3$ (0.5)	**1** (10^{-2})	Et_3N	$FeBr_2$	70	96	57
21 [e]	$CHCl_3$ (0.5)	**1** (10^{-2})	-	$FeBr_2$	120	96	13
22 [e]	$CHCl_3$ (0.5)	**1** (10^{-2})	-	-	120	96	-
23 [e]	$CHCl_3$ (0.5)	-	Et_3N	$FeBr_2$	120	96	-
24 [e]	$CHCl_3$ (0.5)	$Pd(OAc)_2$ (10^{-2})	Et_3N	$FeBr_2$	120	96	86
25 [e]	$CHCl_3$ (0.5)	$Pd(OAc)_2$ (10^{-4})	Et_3N	$FeBr_2$	120	96	<5
26 [c,e]	$CHCl_3$ (0.5)	$Pd(OAc)_2$ (10^{-4})	Et_3N	$FeBr_2$	120	96	-

[a] Reaction conditions: **2a** (0.2 mmol), **3a** (0.2 mmol), base (2 mol%), additive (10^{-2} mol%). [b] Isolated yields. [c] $FeBr_2$ (10^{-4} mol%). [d] **2a** (0.3 mmol), **3a** (0.2 mmol). [e] **2a** (0.2 mmol), **3a** (0.3 mmol).

Figure 2. Palladium-catalyzed formation of benzo[*d*]pyrrolo [2,1-*b*]oxazine-1,5-dione **4a**. Selected optimization experiments [a].

With a catalytic amount (0.01 mol%) of iron(II) bromide as the most favorable additive, an increase in the reaction temperature (120 °C) led to the desired product with a good yield (79%, entry 10). We hypothesized that both the iron Lewis acid and higher temperature favored the key dehydration step. Attempts to decrease the amounts of both the catalyst and the additive (entries 11,12), and to improve the yield by adding a little excess of the alkynoic acid or changing the reaction concentration (entries 13–18) were made so that an excellent 93% yield was obtained by the optimized conditions of entry 17.

Lower temperatures or shorter reaction times (entries 19,20) provided poorer results, and a series of blank experiments proved the need of all the ingredients, including Et_3N as a base and $FeBr_2$ as an additive, along with the palladium source (entries 21–23 vs. 17). In this regard, we were surprised to find that target **4a** was isolated with a yield of 86% when complex **1** was replaced with $Pd(OAc)_2$ (entry 28). Therefore, when the optimized conditions (Figure 2, entry 21) were applied to a number of commercially or readily available (Supplementary Material) alkynoic acids **2** and heterodinucleophiles **3**, $Pd(OAc)_2$ was also evaluated as a catalyst for the reaction.

Benzopyrrolo[1,3]oxazine-1,5-diones and benzopyrido[1,3]oxazine-1,6-diones **4a–e** were prepared in good to excellent yields from anthranilic acid **3a** and several terminal and internal alkynoic acids **2** (Figure 3). In addition to the easy formation of tetracyclic **4c** from *o*-ethynylbenzoic acid and the high diastereoselectivity with which 2-hexylbenzo[*d*]pyrrolo[1,3]oxazine-1,5-dione **4b** was obtained, the use of internal alkyne 5-phenylpent-4-ynoic acid to generate 3a-benzyl derivative **4e**, and the preparation of pyrido[1,3]oxazine-1,6-dione **4d** should be pointed out on account of the reduced reactivity of 5-hexynoic acid in comparison with pentynoic acids [28–30]. An even more interesting observation was that $Pd(OAc)_2$ failed to provide target products **4b–e** in acceptable yields.

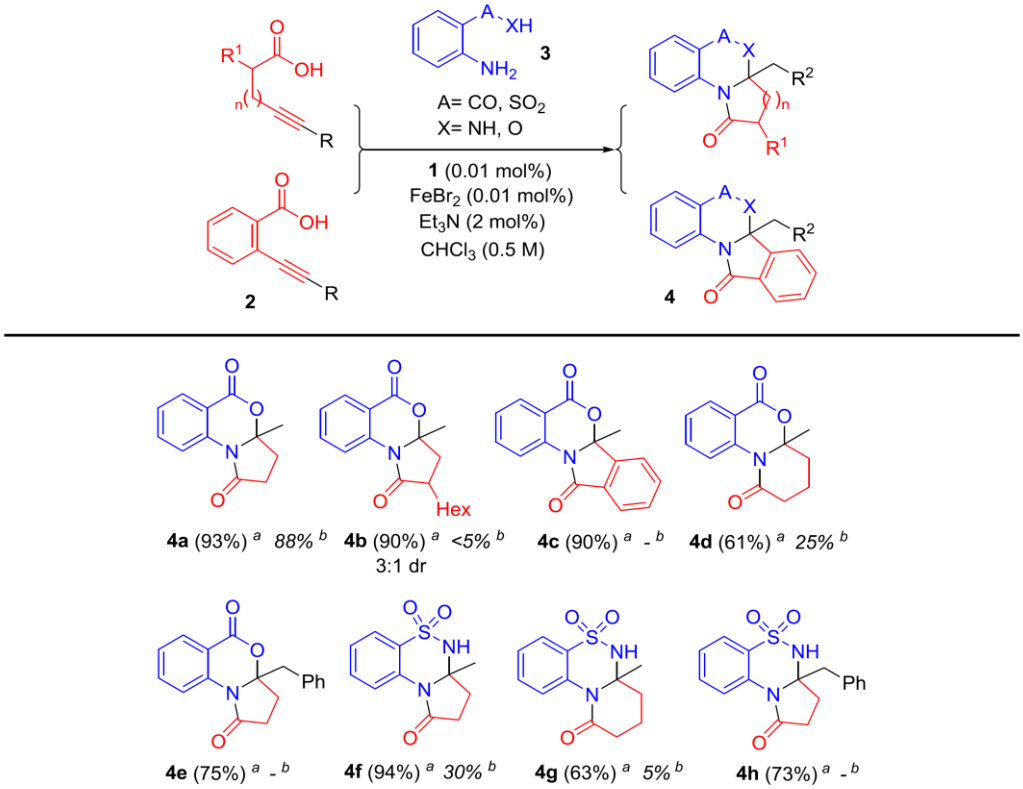

[a] Isolated yield. Reaction conditions: **2** (0.2 mmol), **3** (1.5 equiv.), **1** (10^{-2} mol%), $FeBr_2$ (10^{-2} mol%), Et_3N (2 mol%), $CHCl_3$ (0.4 mL per mmol of **2**), 120 °C, 96 h. [b] Isolated yield. Reaction conditions: **3** (0.2 mmol), **2** (1.5 equiv.), $Pd(OAc)_2$ (10^{-2} mol%), $FeBr_2$ (10^{-2} mol%), Et_3N (2 mol%), $CHCl_3$ (0.4 mL per mmol of **2**), 120 °C, 96 h.

Figure 3. Palladium-catalyzed cascade reaction between alkynoic acids and *o*-aminobenzoic acid or *o*-aminobenzenesulfonamide.

The same trend was observed for the formation of benzopyrrolo[1,2,4]thiadiazin-1-one- and benzopyrido[1,2,4]thiadiazinone-5,5-dioxides **4f–h**, prepared in good to excellent yields only when the system **1**/$FeBr_2$/Et_3N was employed (Figure 3).

Much effort has been devoted to the synthesis of benzopyrrolo[1,2,4]thiadiazine-5,5-dioxides [31–35] due to their nootropic, neuroprotective and cognition-enhancing properties as positive allosteric modulators of the AMPA receptor [36,37]. With regard to **4g**, it is the first benzopyrido[1,2,4]thiadiazinone-5,5-dioxide synthesized so far.

Structure analysis of monocrystals of **4a** and **4e** revealed that both have the same crystal system and space group (orthorrombic Pbca). The presence of the C3a quaternary center (C-11) is responsible for the lack of coplanarity of oxazine and pyrrole rings, as shown by the C1-O1-C11-N1 and C7-N1-C11-C10 torsion angle values of −53.4–39.6° and 165.1–164.4°, respectively. Only the *R* enantiomer of sultam **4g** crystallized in the monoclinic system (Cc) leaving the other C-5 isomer in an amorphous state (Figure 4).

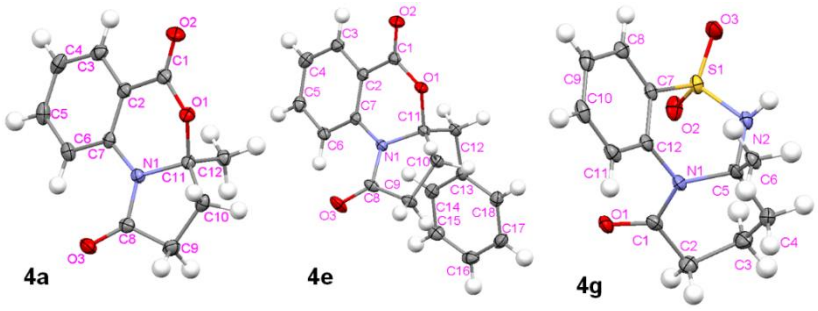

Figure 4. Molecular structure of benzopyrrolo[1,3]oxazine-1,5-diones **4a** and **4e** and benzopyrido[1,2,4]thiadiazinone-5,5-dioxide **4g** with the atomic numbering scheme. Thermal ellipsoids are given at the 50% probability level.

Several diamines **5** were also reacted with alkynoic acids **2**. Palladacycle **1** catalyzed cascade process on a general basis, whereas $Pd(OAc)_2$ did not provide most of the target tri- and tetracycles **6**. In fact, only quinazolinones **6a** and **6c** were obtained when using the latter commercially available palladium source, although with much inferior yields (Figure 5).

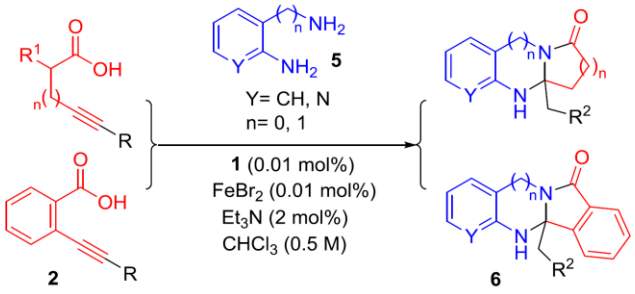

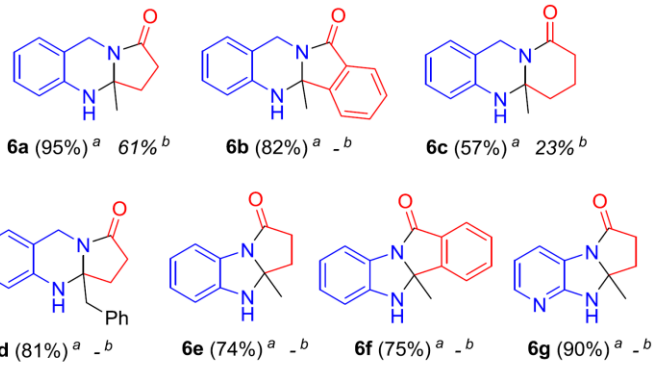

[a] Isolated yield. Reaction conditions: **2** (0.2 mmol), **3** (1.5 equiv.), **1** (10^{-2} mol%), $FeBr_2$ (10^{-2} mol%), Et_3N (2 mol%), $CHCl_3$ (0.4 mL per mmol of **2**), 120 °C, 96 h. [b] Isolated yield. Reaction conditions: **3** (0.2 mmol), **2** (1.5 equiv.), $Pd(OAc)_2$ (10^{-2} mol%), $FeBr_2$ (10^{-2} mol%), Et_3N (2 mol%), $CHCl_3$ (0.4 mL per mmol of **2**), 120 °C, 96 h.

Figure 5. Palladium-catalyzed cascade reaction between alkynoic acids and diamines.

As in the case of derivatives **4**, the reason probably lies in the inability of palladium(II) acetate to catalyze the initial cycloisomerization step at such low catalyst levels. By using remarkably active palladacycle **1**, pyrrolo-, isoindolo- and pyrido[2,1-*b*]quinazolinones **6a–d** were regio-selectively prepared from *o*-aminobenzylamine **5a**. As in the case of anthranilic acid **3a** or 2-aminobenzenesulfonamide **3b**, the use of internal alkynes did not hinder the reaction, and 3a-benzyl derivative **6d** was obtained in good yield. Besides,

reaction of **5a** with 5-hexynoic acid provided pyrido[2,1-*b*]quinazolin-9-one **6c**. So far, this compound had been prepared in reasonable yield only from 5-oxohexanoic acid by a Meyers' lactamization [38].

Benzo[*d*]pyrrolo[1,2-*a*]imidazol-1-one **6a** and benzo[4,5]imidazo[2,1-*a*]isoindol-11-one **6f** (akin to AKR1C3 inhibitor in Figure 1) were prepared by reaction with *o*-phenylene diamine **5b**. Interestingly, a higher yield was obtained for new pyrroloimidazo[4,5-*b*]pyridin-6-one **6g** from 2,3-diaminopyridine **5c**. A significantly greater anticonvulsant effect than currently marketed valproate has been described for several structurally related pyrroloimidazopyridine derivatives prepared by condensation between 2,3-diaminopyridine and 3-acylpropionic acids [39–41]. Considering the latter result from **5c**, a comparison of the reaction yields from dinucleophiles **3a**,**b** and **5a**–**c** with 4-pentynoic acid **2a** led to the conclusion that the reaction is favored by the use of non-symmetric dinucleophiles.

Several experiments were then carried out in order to shed light on the role of complex **1** in the reaction mechanism. Taking the reaction leading to the formation of benzopyrrolo[1,3]oxazine-1,5-dione **4a** as a model example, a plot of the conversion of anthranilic acid **3a** vs. time showed neither sigmoidal shape nor induction time (Figure 6).

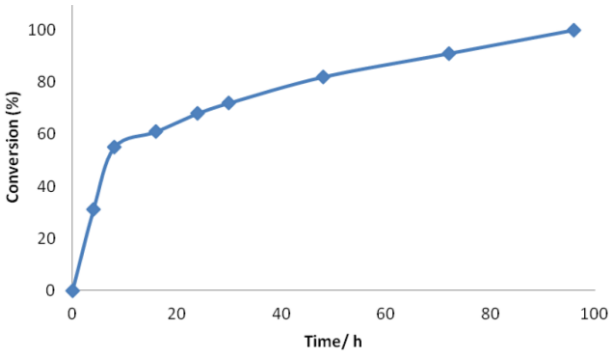

Figure 6. Conversion rate of anthranilic acid 3a versus time.

In addition, the latter reaction was also conducted in the presence of substoichiometric and overstoichiometric amounts of a number of known poisoning agents for palladium nanoparticles and other palladium(0) heterogeneous catalysts, including the mercury drop test (Table 1). Not the slightest inhibition or poisoning effect was observed in our case, as expected for a fully homogeneous catalyst system [42–47].

Table 1. Summary of poisoning experiments [a].

Entry	Poisoning Additive	4a (%) [b]
1	Hg (one drop)	99
2	CS_2 (0.5 equiv. per metal atom)	99
3	CS_2 (2.0 equiv. per metal atom)	98
4	PPh_3 (0.03 equiv. per metal atom)	99
5	PPh_3 (0.3 equiv. per metal atom)	99
6	PPh_3 (4.0 equiv. per metal atom)	99
7	Py (150 equiv. per metal atom) [c]	98
8	PVPy (300 equiv. per metal atom) [d]	99

[a] Reaction conditions: **3a** (0.2 mmol), **2a** (1.5 equiv.), **1** (10^{-2} mol%), $FeBr_2$ (10^{-2} mol%), Et_3N (2 mol%), $CHCl_3$ (0.4 mL per mmol of **2**), 120 °C, 96 h. [b] NMR yields determined using 3,4,5-trichloropyridine as an internal standard. [c] Py: Pyridine. [d] PVPy: Polyvinylpyridine.

Moreover, transmission electron microscopy (TEM) analysis of the reaction mixture from **3a** + **2a** -> **4a**, combined with energy dispersive X-ray microanalysis revealed the presence of some scattered iron nanoparticles (average size 8 nm) but no trace of palladium nanoparticles (Figure 7).

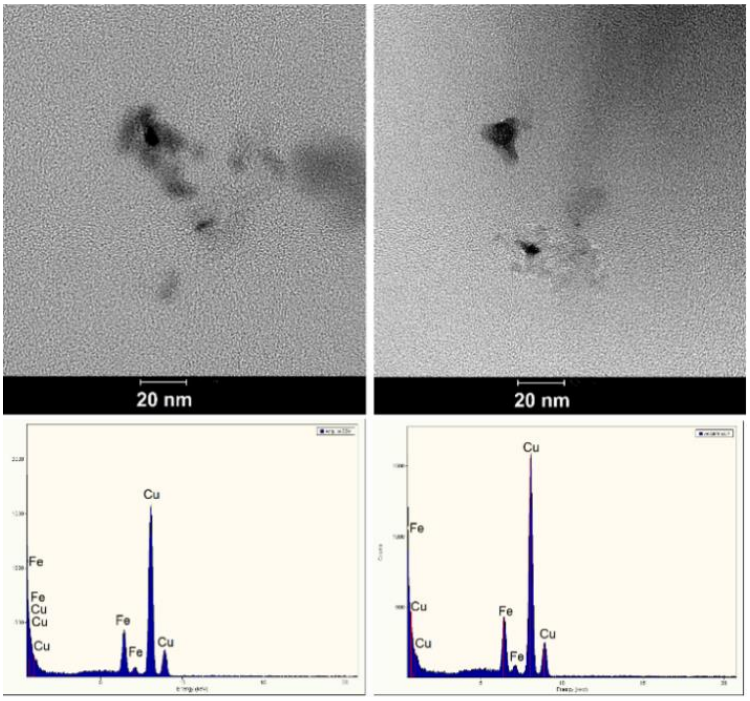

Figure 7. TEM images and EDX spectra of the crude. Note: The presence of copper is due to the grid supporting the sample.

UPLC-ESI analysis of a sample taken from the reaction mixture (**2a** + **3a** -> **4a**) after 12 h of reaction not only provided evidence of the presence of several transient intermediates related to the ones postulated in Scheme 1, but also of the participation of a number of palladium and iron species displayed in Scheme 2 (see Supplementary Material for further details), thus supporting our hypothesis on the crucial role of such ingredients in the cascade reaction. On the basis of the detection of the above intermediates, a revised catalytic cycle was tentatively proposed (Scheme 2). Interaction of alkynoic acid **2a** with cationic **1′** to form complex **A** activates the alkyne for the triethylamine-promoted cycloisomerization process that generates intermediate **B**, which upon protonation and interaction with Lewis's acids **1′** and $FeBr_2$ produces transient species **C**. Ring-opening amidation with *o*-amino derivative **3a** leads to activated ketoamides **D**, which upon cyclization form hydroxypyrrolidinones **E**. After dehydration, the resulting *N*-acyliminium intermediates **F** undergo a final lactamization step to provide oxazinanone derivative **4a**. According to the transient species detected by ESI-mass spectrometry (Supplementary Material), it seems that although the palladium catalyst is essential to initiate the cycloisomerization step and thus to promote the reaction, the iron additive facilitates several nucleophilic addition and dehydration steps via Lewis acid activation.

Finally, methylidene lactone **7** was prepared using catalyst **1**, and then reacted with anthranilic acid **3a** in the presence and absence of the optimized catalyst and additives. Target benzopyrrolo[1,3]oxazine-1,5-dione **4a** was obtained in good yield (90%, Scheme 3) only when both complex **1** and $FeBr_2$ were employed, whereas reactions lacking any of these ingredients led to negligible results (yield of **4a** < 15%) (see Supplementary Material for further details), thus offering further support for the proposed reaction pathway.

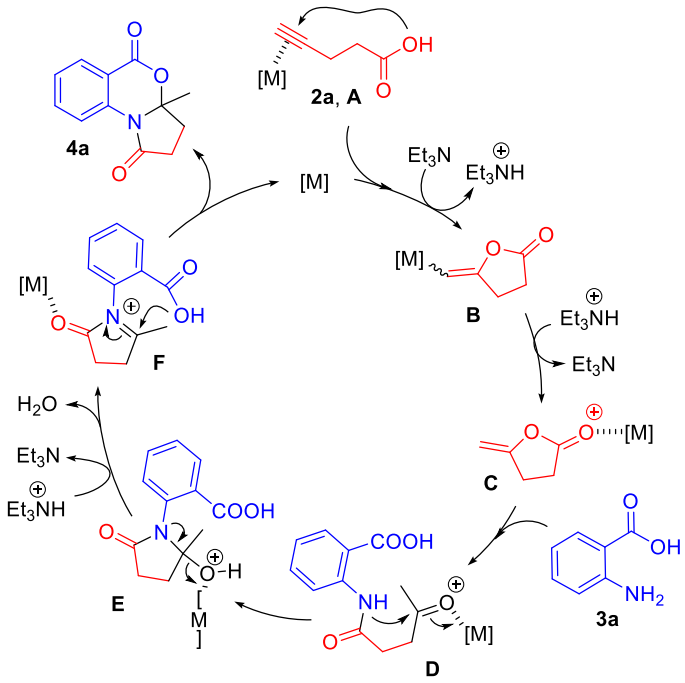

Scheme 2. Revised catalytic cycle for the cascade reaction catalyzed by the **1**/$FeBr_3$/Et_3N system.

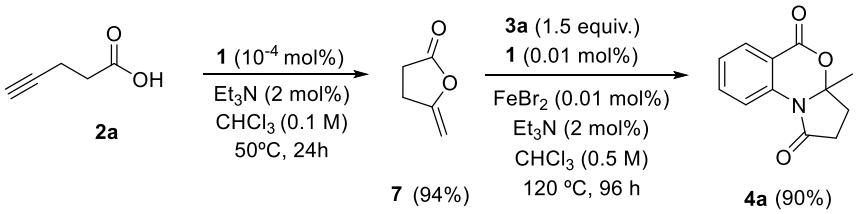

Scheme 3. Reaction of methylene lactone **7** with anthranilic acid **3a** under optimized conditions.

3. Materials and Methods

3.1. General Information

Commercially available reagents were used throughout without purification unless otherwise stated. ^1H and ^{13}C NMR spectra were recorded on a Bruker AC-300 instrument (300 MHz for ^1H and 75.4 MHz for ^{13}C) at 20 °C. Chemical shifts (d) are given in ppm downfield from Me_4Si and are referenced as internal standard to the residual solvent (unless indicated) $CDCl_3$ (d = 7.26 for ^1H and d = 77.00 for ^{13}C). Coupling constants, J, are reported in hertz (Hz). Melting points were determined in a capillary tube and are uncorrected. TLC was carried out on SiO_2 (silica gel 60 F254, Merck), and the spots were located with UV light. Flash chromatography was carried out on SiO_2 (silica gel 60, Merck, 230–400 mesh ASTM). Drying of organic extracts during work-up of reactions was performed over anhydrous Na_2SO_4. Evaporation of solvents was accomplished with a Büchi rotatory evaporator. MS spectra were recorded on an Agilent 5975 mass spectrometer under electronic impact (EI) conditions or on an Acquity UPLC-Spectrometer of Mass QTOF from Waters under electrospray ionization (ESI). HRMS were recorded using a Micromass GCT spectrometer by electronic impact (EI) or electrospray ionization (ESI). Single crystal X-ray intensity data were collected on an Agilent Technologies Super-Nova diffractometer, which was equipped with monochromated Cu kα radiation (λ = 1.54184 A) and Atlas CCD detector. A measurement was carried out at 100(2) K with the help of an Oxford Cryostream 700 PLUS temperature device. Data frames were processed (united cell determination, analytical absorption correction with face indexing, intensity data integration and correction for Lorentz and polarization effects) using the Crysalis software package [48]. The structure was solved using Olex2 [49] and refined by full-matrix least-squares with SHELXL-97 [50].

Final geometrical calculations were carried out with Mercury [51] and PLATON [52] as integrated in WinGX [53].

3.2. General Procedure for Complex 1-Catalyzed Cascade Reaction between Alkynoic Acids and Heterodinucleophiles

Alkynoic acid **2** (0.2 mmol) and heterodinucleophile **3** or **5** (0.3 mmol) were charged in a heavy-wall pressure tube at room temperature with a magnetic stir bar under argon. Then, triethylamine (0.56 µL, 4.0×10^{-3} mmol), a solution of $FeBr_2$ (30 µL of a 0.67 M solution in $CHCl_3$, 2×10^{-5} mmol), a solution of NNC pincer **1** (30 µL of a 0.67 M solution in $CHCl_3$, 2×10^{-5} mmol) and $CHCl_3$ (0.34 mL) were added, the tube closed, and the mixture was heated in an oil bath at 120 °C for 96 h. After cooling, the mixture was concentrated *in vacuo* and purified by flash column chromatography using hexane/ethyl acetate as eluent to provide polycyclic compounds **4**/**6**.

3a-Methyl-3,3a-dihydro-5*H*-benzo[*d*]pyrrolo[2,1-*b*][1,3]oxazine-1,5(2*H*)-dione (**4a**). The general procedure was followed, and compound **4a** was obtained as colorless prisms (40.4 mg, 93%). m.p. 143–147 °C ($CHCl_3$)(Lit. [10] 165–167 °C); Its NMR spectra were consistent with published data [10]. ^{1}H NMR ($CDCl_3$) δ 8.12–8.05 (m, 2H, H_{arom}), 7.71–7.65 (m, 1H, H_{arom}), 7.34 (t, *J* = 7.7 Hz, 1H, H_{arom}), 2.84–2.37 (m, 4H, CH_2), 1.70 (s, 3H, CH_3). ^{13}C NMR ($CDCl_3$) δ 171.6 (NCO), 161.6 (COO), 136.2 (qC_{arom}), 135.5, 130.4, 125.8, 121.1 (C_{arom}), 116.3 (qC_{arom}), 95.34 (qC), 32.3 (CH_2), 29.4 (CH_2), 24.8 (CH_3).

2-Hexyl-3a-methyl-3,3a-dihydro-1*H*-benzo[*d*]pyrrolo[2,1-*b*][1,3]oxazine-1,5(2*H*)-dione, (**4b**). The general procedure was followed, and compound **4b** was obtained as a mixture of diasteroisomers (3:1) which were separated by flash column chromatography using Hexanes:EtOAc 8:2 as eluent. Their NMR spectra were consistent with published data [10]. Diasteroisomer **4ba**, colorless oil (36.3 mg, 70%); ^{1}H NMR ($CDCl_3$) δ 8.15 (d, *J* = 8.2 Hz, 1H, H_{arom}), 8.09 (dd, *J* = 7.9, 1.4 Hz, 1H, H_{arom}), 7.67 (td, *J* = 8.2, 1.5 Hz, 1H, H_{arom}), 7.38–7.20 (m, 1H, H_{arom}), 2.75–2.52 (m, 2H, CH_2), 2.19–2.27 (m, 1H, CH), 2.07–1.91 (m, 1H, CH_2), 1.67 (s, 3H, CH_3), 1.41–1.25 (m, 9H, H_{alkil}), 0.87 (m, 3H, CH_3); ^{13}C NMR ($CDCl_3$) δ 173.2 (NCO), 161.5 (COO), 136.2 (qC_{arom}), 135.5, 130.4, 125.3, 120.3 (C_{arom}), 115.6 (qC_{arom}), 93.4 (qC), 40.7 (CH_2), 39.2 (CH), 31.5 (CH_2), 30.4 (CH_2), 29.0 (CH_2), 26.8 (CH_2), 24.3 (CH_2), 22.5 (CH_3), 13.9 (CH_3). Diasteroisomer **4bb**, yellow oil (12.7 mg, 20%); ^{1}H NMR ($CDCl_3$) δ 8.10 (dd, *J* = 7.8, 1.3 Hz, 1H, H_{arom}), 7.85 (d, *J* = 8.1 Hz, 1H, H_{arom}), 7.69 (td, *J* = 8.0, 1.5 Hz, 1H, H_{arom}), 7.35 (td, *J* = 7.7, 1.0 Hz, 1H, H_{arom}), 2.88–2.71 (m, 2H, H_{arom}), 2.09–2.08 (m, 1H, CH), 2.04–1.89 (m, 1H, CH_2), 1.71 (s, 3H, CH_3), 1.38–1.25 (m, 9H, H_{alkil}), 0.90 (t, *J* = 6.4 Hz, 3H, CH_3); ^{13}C NMR ($CDCl_3$) δ 175.4 (NCO), 162.0 (COO), 136.4 (qC_{arom}), 153.2, 130.2, 126.1, 122.5 (C_{arom}), 117.7 (qC_{arom}), 94.6 (qC), 40.6 (CH_2), 38.2 (CH), 31.8 (CH_2), 31.6 (CH_2), 28.9 (CH_2), 27.1 (CH_2), 26.2 (CH_2), 22.5 (CH_3), 14.0 (CH_3).

6a-Methyl-5*H*-benzo[4,5][1,3]oxazino[2,3-*a*]isoindole-5,11(6a*H*)-dione (**4c**). The general procedure was followed, and compound **4c** was obtained as a yellow powder (46.1 mg, 87%); m.p. 138–142 °C ($CHCl_3$)(Lit. [54] 145–148 °C (^{i}PrOH)); Its NMR spectra were consistent with published data [15]. ^{1}H NMR ($CDCl_3$) δ 8.16 (dd, *J* = 7.9, 1.3 Hz, 1H, H_{arom}), 8.12 (d, *J* = 8.2 Hz, 1H, H_{arom}), 7.96 (d, *J* = 7.5 Hz, 1H, H_{arom}), 7.81–7.71 (m, 3H, H_{arom}), 7.68–7.61 (m, 1H, H_{arom}), 7.40–7.35 (m, 1H, H_{arom}), 1.95 (s, 3H, CH_3); ^{13}C-NMR ($CDCl_3$) δ 164.7 (NCO), 162.0 (COO), 144.20, 136.2 (qC_{arom}), 135.8, 133.9, 130.9, 130.6 (C_{arom}), 130.0 (qC_{arom}), 125.5, 124.7, 122. 5, 121.4 (C_{arom}), 115.6 (qC_{arom}), 92.6 (qC), 24.3 (CH_3).

4a-Methyl-2,3,4,4a-tetrahydro-1*H*,6*H*-benzo[d]pyrido[2,1-*b*][1,3]oxazine-1,6-dione (**4d**). The general procedure was followed, and compound **4d** was obtained as a white powder (28.8 mg, 61%); m.p. 70–72 °C ($CHCl_3$)(Lit. [10] 66–68 °C); Its NMR spectra were consistent with published data [10]. ^{1}H NMR ($CDCl_3$) δ 8.06 (dd, *J* = 7.8, 1.5 Hz, 1H, H_{arom}), 7.78 (dd, *J* = 8.0, 0.9 Hz, 1H, H_{arom}), 7.64 (td, *J* = 7.8, 1.5 Hz, 1H, H_{arom}), 7.35 (td, *J* = 8.0, 0.9 Hz, 1H, H_{arom}), 2.72–2.53 (m, 2H, CH_2), 2.49–2.35 (m, 1H, CH_2), 2.21–2.01 (m, 2H, CH_2), 1.96–1.79 (m, 1H, CH_2), 1.62 (s, 3H, CH_3); ^{13}C NMR ($CDCl_3$) δ 169.2 (NCO), 162.5 (COO), 138.6

(qC_{arom}), 134.1, 129.3, 126.2, 126.1 (C_{arom}), 120.3 (qC_{arom}), 92.4 (qC), 36.0 (CH_2), 33.4 (CH_2), 26.7 (CH_2), 16.6 (CH_3).

3a-Benzyl-3,3a-dihydro-5*H*-benzo[*d*]pyrrolo[2,1-*b*][1,3]oxazine-1,5(2*H*)-dione (**4e**). The general procedure was followed, and compound **4e** was obtained as colorless prisms (43.9 mg, 75%); m.p. 142–146 °C ($CHCl_3$); ^{1}H NMR ($CDCl_3$) δ 8.21 (d, *J* = 8.0 Hz, 1H, H_{arom}), 8.14 (dd, *J* = 7.8, 1.4 Hz, 1H, H_{arom}), 7.77 (td, *J* = 8.2, 1.5 Hz, 1H, H_{arom}), 7.37 (td, *J* = 7.8, 0.9 Hz, 1H, H_{arom}), 7.28 (dd, *J* = 6.6, 3.9 Hz, 3H, H_{arom}), 7.04 (dd, *J* = 6.5, 2.9 Hz, 2H, H_{arom}), 3.36 (d, *J* = 13.8 Hz, 1H, CH_2), 3.11 (d, *J* = 13.7 Hz, 1H, CH_2), 2.65–2.29 (m, 3H, CH_2), 1.73–1.50 (m, 1H, CH_2); ^{13}C NMR ($CDCl_3$) δ 172.0 (NCO), 161.4 (COO), 136.3 (qC_{arom}), 135.9 (C_{arom}), 133.0 (qC_{arom}), 130.6, 129.9, 128.9, 127.9, 125.8, 120.7 (C_{arom}), 116.3 (qC_{arom}), 96.8 (qC), 42.6 (CH_2), 30.2 (CH_2), 29.5 (CH_2); HRMS (*m*/*z*): $[M + H]^+$ calc. for $C_{18}H_{16}NO_3$: 294.1130; found: 294.1129.

3a-Methyl-2,3,3a,4-tetrahydro-1*H*-benzo[*e*]pyrrolo[2,1-*c*][1,2,4]thiadiazin-1-one 5,5-dioxide (**4f**). The general procedure was followed, and compound **4f** was obtained as colorless prisms (47.4 mg, 94%); m.p. 189–192 °C ($CHCl_3$); ^{1}H NMR (DMSO-d_6) 8.55 (s, 1H, NH), 8.28 (dd, *J* = 8.4, 0.8 Hz, 1H, H_{arom}), 7.81 (dd, *J* = 7.9, 1.4 Hz, 1H, H_{arom}), 7.73–7.55 (m, 1H, H_{arom}), 7.38 (td, *J* = 7.8, 1.0 Hz, 1H, H_{arom}), 2.77 (dt, *J* = 17.2, 10.0 Hz, 1H, CH_2), 2.31–2.18 (m, 3H, CH_2), 1.58 (s, 3H, CH_3); ^{13}C NMR (DMSO-d_6) δ 172.3 (NCO), 133.6 (C_{arom}), 132.9, 127.9 (qC_{arom}), 125.6, 124.7, 122.2 (C_{arom}), 78.1 (qC), 33.2 (CH_2), 29.6 (CH_2), 24.5 (CH_3); HRMS (*m*/*z*): $[M + H]^+$ calc. for $C_{11}H_{13}N_2O_3S$: 253.0647; found: 253.0640.

6a-Methyl-6a,7,8,9-tetrahydrobenzo[*e*]pyrido[2,1-*c*][1,2,4]thiadiazin-10(6*H*)-one 5,5-dioxide (**4g**). The general procedure was followed, and compound **4g** was obtained as yellow prisms (33.5 mg, 63%); m.p. 196–199 °C ($CHCl_3$); ^{1}H NMR ($CDCl_3$) δ 7.81 (d, *J* = 7.7 Hz, 1H, H_{arom}), 7.58 (d, *J* = 3.7 Hz, 2H, H_{arom}), 7.44–7.36 (m, 1H, H_{arom}), 5.17 (bs, 1H, NH), 2.62 (t, *J* = 6.3 Hz, 2H, CH_2), 2.23–2.06 (m, 3H, CH_2), 1.95–1.80 (m, 1H, CH_2), 1.52 (s, 3H, CH_3); ^{13}C NMR ($CDCl_3$) δ 170.0 (NCO), 135.4 (qC_{arom}), 134.5 (qC_{arom}), 132.4, 129.3, 127.0, 123.4 (C_{arom}), 76.1 (qC), 38.1, 33.3 (CH_2), 27.6 (CH_3), 16.2 (CH_2); HRMS (*m*/*z*): $[M + H]^+$ calc. for $C_{12}H_{15}N_2O_3S$: 267.0803; found: 267.0802.

3a-Benzyl-2,3,3a,4-tetrahydro-1*H*-benzo[*e*]pyrrolo[2,1-*c*][1,2,4]thiadiazin-1-one 5,5-dioxide (**4h**). The general procedure was followed, and compound **4h** was obtained as a white powder (47.9 mg, 73%); m.p. 194–196 °C ($CHCl_3$); ^{1}H NMR ($CDCl_3$) δ 8.32 (d, *J* = 8.4 Hz, 1H, H_{arom}), 7.80 (d, *J* = 7.9 Hz, 1H, H_{arom}), 7.61 (t, *J* = 7.4 Hz, 1H, H_{arom}), 7.26–7.30 (m, 4H, H_{arom}), 7.04–7.07 (m, 2H, H_{arom}), 5.77 (bs, 1H, NH), 3.54 (d, *J* = 14.1 Hz, 1H, CH_2), 3.06 (d, *J* = 14.1 Hz, 1H, CH_2), 2.55–2.46 (m, 1H, CH_2), 2.24–1.99 (m, 2H, CH_2), 1.46–1.31 (m, 1H, CH_2); ^{13}C NMR ($CDCl_3$) δ 172.4 (NCO), 133.7 (C_{arom}), 132.5 (qC_{arom}), 130.1, 128.9 (C_{arom}), 127.9 (qC_{arom}), 127.8, 125.8, 124.7, 122.8 (C_{arom}), 80.3 (qC), 42.1 (CH_2), 31.3 (CH_2), 29.6 (CH_2); HRMS (*m*/*z*): $[M + H]^+$ calc. for $C_{17}H_{17}N_2O_3S$: 329.0960; found: 329.0957.

3a-Methyl-3,3a,4,9-tetrahydropyrrolo[2,1-*b*]quinazolin-1(2*H*)-one (**6a**). The general procedure was followed, and compound **6a** was obtained as yellow prisms (38.4 mg, 95%); m.p. 131–134 °C ($CHCl_3$)(Lit. [8] 138–140 °C); Its NMR spectra were consistent with published data [8]. ^{1}H NMR ($CDCl_3$) δ 7.10–6.96 (m, 1H, H_{arom}), 6.78 (t, *J* = 7.4 Hz, 1H, H_{arom}), 6.56 (d, *J* = 8.0 Hz, 1H, H_{arom}), 5.02 (d, *J* = 16.9 Hz, 1H, CH_2), 4.17 (d, *J* = 16.8 Hz, 1H, CH_2), 3.83 (bs, 1H, NH), 2.59–2.48 (m, 2H, CH_2), 2.25–1.97 (m, 2H, CH_2), 1.54 (s, 3H, CH_3); ^{13}C NMR ($CDCl_3$) δ 174.2 (NCO), 141.8 (qC_{arom}), 127.6, 126.9, 119.3 (C_{arom}), 117.4 (qC_{arom}), 116.4 (C_{arom}), 71.9 (qC), 38.6 (CH_2), 32.9 (CH_2), 29.5 (CH_2), 25.6 (CH_3).

4b-Methyl-5,10-dihydroisoindolo[1,2-*b*]quinazolin-12(4b*H*)-one (**6b**). The general procedure was followed, and compound **6b** was obtained as a brown powder (41.0 mg, 82%); m.p. 190–194 °C ($CHCl_3$)(Lit. [8] 222–224 °C); Its NMR spectra were consistent with published data [8]. ^{1}H NMR ($CDCl_3$) δ 7.88 (d, *J* = 7.4 Hz, 2H, H_{arom}), 7.63 (d, *J* = 4.0 Hz, 2H, H_{arom}), 7.58–7.48 (m, 1H, H_{arom}), 7.15–7.09 (m, 2H, H_{arom}), 6.88 (t, *J* = 7.4 Hz, 1H, H_{arom}), 6.69 (d, *J* = 8.0 Hz, 1H, H_{arom}), 5.32 (d, *J* = 16.8 Hz, 1H, CH_2), 4.45 (d, *J* = 17.1 Hz, 1H, CH_2),

1.71 (s, 3H, CH_3); ^{13}C NMR ($CDCl_3$) δ 165.7 (NCO), 147.7, 140.0 (qC_{arom}), 132.2 (C_{arom}), 131.3 (qC_{arom}), 129.5, 127.8, 127.1, 124.3, 120.5, 120.3 (C_{arom}), 118.6 (qC_{arom}), 118.0 (C_{arom}), 71.4 (qC), 37.9 (CH_2), 23.8 (CH_3).

5a-Methyl-5,5a,6,7,8,11-hexahydro-9*H*-pyrido[2,1-*b*]quinazolin-9-one (**6c**). The general procedure was followed, and compound **6c** was obtained as a yellow powder (24.6 mg, 57%); m.p. 135–138 °C ($CHCl_3$)(Lit. [8] 156–158 °C); Its NMR spectra were consistent with published data [8]. ^1H NMR ($CDCl_3$) δ 7.05 (d, *J* = 7.8 Hz, 2H, H_{arom}), 6.79 (t, *J* = 7.4 Hz, 1H, H_{arom}), 6.60 (d, *J* = 7.8 Hz, 1H, H_{arom}), 5.48 (d, *J* = 17.3 Hz, 1H, CH_2), 4.18 (d, *J* = 17.3 Hz, 1H, CH_2), 2.60–2.29 (m, 2H, CH_2), 2.09–1.86 (m, 3H, CH_2), 1.84–1.68 (m, 1H, CH_2), 1.53 (s, 3H, CH_3); ^{13}C NMR ($CDCl_3$) δ 169.0 (NCO), 141.0 (qC_{arom}), 127.4, 126.8, 119.3 (C_{arom}), 118.9 (qC_{arom}), 116.1 (C_{arom}), 68.3 (qC), 39.8 (CH_2), 37.4 (CH_2), 32.9 (CH_2), 26.9 (CH_2), 16.8 (CH_3).

3a-Benzyl-3,3a,4,9-tetrahydropyrrolo[2,1-*b*]quinazolin-1(2*H*)-one (**6d**). The general procedure was followed, and compound **6d** was obtained as an orange oil (45.0 mg, 81%); ^1H NMR ($CDCl_3$) δ 7.26–7.35 (m, 3H, H_{arom}), 7.17–7.03 (m, 4H, H_{arom}), 6.83 (t, *J* = 7.4 Hz, 1H, H_{arom}), 6.59 (d, *J* = 7.8 Hz, 1H, H_{arom}), 5.11 (d, *J* = 17.1 Hz, 1H, CH_2), 4.34 (d, *J* = 17.1 Hz, 1H, CH_2), 4.04 (bs, 1H, NH), 3.22 (d, *J* = 13.1 Hz, 1H, CH_2), 2.90 (d, *J* = 13.1 Hz, 1H, CH_2), 2.54–2.18 (m, 3H, CH_2), 1.84–1.62 (m, 1H, CH_2); ^{13}C NMR ($CDCl_3$) δ 174.6 (NCO), 141.4 (qC_{arom}), 135.5 (qC_{arom}), 130.1, 128.7, 127.9, 127.3, 127.1, 119.4 (C_{arom}), 117.5 (qC_{arom}), 116.3 (C_{arom}), 74.1 (qC), 42.5 (CH_2), 39.1 (CH_2), 30.5 (CH_2), 29.3 (CH_2); HRMS (*m*/*z*): $[M + H]^+$ calc. for $C_{18}H_{19}N_2O$: 279.1497; found: 279.1498.

3a-Methyl-2,3,3a,4-tetrahydro-1*H*-benzo[*d*]pyrrolo[1,2-*a*]imidazol-1-one (**6e**). The general procedure was followed, and compound **6e** was obtained as a brown oil (27.8 mg, 74%); Its NMR spectra were consistent with published data [40]. ^1H NMR ($CDCl_3$) δ 7.45 (dd, *J* = 7.6, 0.8 Hz, 1H, H_{arom}), 6.98 (td, *J* = 7.7, 1.2 Hz, 1H, H_{arom}), 6.84 (td, *J* = 7.6, 1.1 Hz, 1H, H_{arom}), 6.70 (dd, *J* = 7.7, 0.6 Hz, 1H, H_{arom}), 4.20 (bs, 1H, NH), 2.87–2.74 (m, 1H, CH_2), 2.61–2.47 (m, 1H, CH_2), 2.45–2.36 (m, 2H, CH_2), 1.53 (s, 3H, CH_3); ^{13}C NMR ($CDCl_3$) δ 173.7 (NCO), 142.7, 128.6 (qC_{arom}), 125.2, 120.1, 115.4, 110.6 (C_{arom}), 85.6 (qC), 37.7 (CH_2), 33.6 (CH_2), 26.2 (CH_3).

4b-Methyl-4b,5-dihydro-11*H*-benzo[4,5]imidazo[2,1-*a*]isoindol-11-one (**6f**). The general procedure was followed, and compound **6f** was obtained as a yellow powder (41.5 mg, 75%); m.p. 146–149 °C ($CHCl_3$)(Lit. [55] 184–185 °C); Its NMR spectra were consistent with published data [55]. ^1H NMR ($CDCl_3$) δ 7.86 (d, *J* = 8.1 Hz, 1H, H_{arom}), 7.63 (t, *J* = 7.4 Hz, 1H, H_{arom}), 7.57–7.47 (m, 3H, H_{arom}), 7.03–6.87 (m, 2H, H_{arom}), 6.74 (d, *J* = 7.7 Hz, 1H, H_{arom}), 4.24 (s, 1H, NH), 1.83 (s, 3H, CH_3); ^{13}C NMR ($CDCl_3$) δ 170.6 (NCO), 149.5, 145.0 (qC_{arom}), 133.4 (C_{arom}), 132.1, 130.7 (qC_{arom}), 129.6, 125.3, 125.1, 121.8, 121.1, 117.2, 111.5 (C_{arom}), 86.0 (qC), 26.8 (CH_3).

8a-Methyl-7,8,8a,9-tetrahydro-6*H*-pyrrolo[1′,2′:1,2]imidazo[4,5-*b*]pyridin-6-one (**6g**). The general procedure was followed, and compound **6g** was obtained as a brown oil (34.0 mg, 90%); Its NMR spectra were consistent with published data [40]. ^1H NMR ($CDCl_3$) δ 7.75 (dd, *J* = 5.4, 1.2 Hz, 1H, H_{arom}), 7.52 (dd, *J* = 7.4, 1.4 Hz, 1H, H_{arom}), 6.66 (dd, *J* = 7.4, 5.5 Hz, 1H, H_{arom}), 5.84 (bs, 1H, NH), 2.87–2.65 (m, 1H, CH_2), 2.60–2.38 (m, 3H, CH_2), 1.58 (s, 3H, CH_3); ^{13}C NMR ($CDCl_3$) δ 174.9 (NCO), 156.6 (qC_{arom}), 142.8 (C_{arom}), 122.5 (qC_{arom}), 120.6, 114.5 (C_{arom}), 83.3 (qC), 38.2 (CH_2), 32.5 (CH_2), 26.7 (CH_3).

4. Conclusions

To sum up, an alternative catalyst system for the cascade reaction between alkynoic acids and heterodinucleophiles is presented. This palladium-based system is based on the use of very small amounts of a NNC pincer complex, thus providing a more efficient approach to polycyclic structures of interest. Good to excellent yields are obtained in all cases by this particularly active system, which according to a number of mechanistic studies

participates as a fully homogenous catalyst. A more nuanced mechanism describing the role of the metal species and transient intermediates detected by UPLC-ESI is also proposed.

Supplementary Materials: The following are available online at https://www.mdpi.com/article/10.3390/catal12020127/s1, synthesis of 5-phenylpent-4-ynoic acid, structure factor tables, additional experiments, ESI-MS results and scans of NMR spectra (PDF).

Author Contributions: Co-authors M.T.H., N.C. and G.U. contributed to searching and collating of the relevant literature and the proof-reading of the document. Investigation, experiments and analysis were carried out by N.C. Corresponding author R.S. conceptualized and supervised the study and wrote the body of the article. All authors have read and agreed to the published version of the manuscript.

Funding: This research was funded by the Basque Government (IT1405-19) and the Spanish Ministry of Economy and Competitiveness (CTQ2017-86630-P).

Acknowledgments: Technical and human support provided by SGIker of UPV/EHU is gratefully acknowledged.

Conflicts of Interest: The authors declare no conflict of interest.

References

1. Gopalaiah, K.; Choudhary, R. Synthesis of Kröhnke pyridines through iron-catalyzed oxidative condensation/double alkynylation/amination cascade strategy. *Tetrahedron* **2021**, *98*, 132429. [CrossRef]
2. Liao, X.R.; Zhou, F.L.; Bin, Z.Y.; Yang, Y.D.; You, J.S. Palladium-Catalyzed Cascade Dearomative Spirocyclization and C-H Annulation of Aromatic Halides with Alkynes. *Org. Lett.* **2021**, *23*, 5203–5207. [CrossRef]
3. Yang, X.H.; Huang, J.; Wang, F.; Liu, Z.L.; Li, Y.J.; Tao, C.A.; Wang, J.F. Copper-catalyzed alkynylation/annulation cascades of N-allyl ynamides: Regioselective access to medium-sized N-heterocycles. *Org. Chem. Front.* **2021**, *8*, 18–24. [CrossRef]
4. Yang, Y.Z.; He, D.L.; Li, J.H. Rhodium-Catalyzed Reductive trans-Alkylacylation of Internal Alkynes via a Formal Carborhodation/C-H Carbonylation Cascade. *Org. Lett.* **2021**, *23*, 5039–5043. [CrossRef] [PubMed]
5. Yang, T.; Campbell, L.; Dixon, D.J. A Au(I)-Catalyzed N-Acyl Iminium Ion. Cyclization Cascade. *J. Am. Chem. Soc.* **2007**, *129*, 12070–12071. [CrossRef]
6. Muratore, M.E.; Holloway, C.A.; Pilling, A.W.; Storer, R.I.; Trevitt, G.; Dixon, D.J. Enantioselective Brønsted Acid-Catalyzed N-Acyliminium Cyclization Cascades. *J. Am. Chem. Soc.* **2009**, *131*, 10796–10797. [CrossRef]
7. Yang, T.; Ferrali, A.; Campbell, L.; Dixon, D.J. Combination iminium, enamine and copper(I) cascade catalysis: A carboannulation for the synthesis of cyclopentenes. *Chem. Commun.* **2008**, *25*, 2923–2925. [CrossRef] [PubMed]
8. Patil, N.T.; Mutyala, A.K.; Lakshmi, P.G.V.; Gajula, B.; Sridhar, B.; Pottireddygari, G.R.; Rao, T.P. Au(I)-Catalyzed Cascade Reaction Involving Formal Double Hydroamination of Alkynes Bearing Tethered Carboxylic Groups: An Easy Access to Fused Dihydrobenzimidazoles and Tetrahydroquinazolines. *J. Org. Chem.* **2010**, *75*, 5963–5975. [CrossRef]
9. Patil, N.T.; Shinde, V.S.; Sridhar, B. Relay Catalytic Branching Cascade: A Technique to Access Diverse Molecular Scaffolds. *Angew. Chem. Int. Ed.* **2013**, *52*, 2251–2255. [CrossRef]
10. Feng, E.; Zhou, Y.; Zhang, D.; Zhang, L.; Sun, H.; Jiang, H.; Liu, H. Gold(I)-Catalyzed Tandem Transformation: A Simple Approach for the Synthesis of Pyrrolo/Pyrido[2,1-*a*][1,3]benzoxazinones and Pyrrolo/Pyrido[2,1-a]quinazolinones. *J. Org. Chem.* **2010**, *75*, 3274–3282. [CrossRef]
11. Zhou, Y.; Zhai, Y.; Ji, X.; Liu, G.; Feng, E.; Ye, D.; Zhao, L.; Jiang, H.; Liu, H. Gold(I)-Catalyzed One-Pot Tandem Coupling/Cyclization: An Efficient Synthesis of Pyrrolo-/Pyrido[2,1-*b*]benzo[*d*][1,3]oxazin-1-ones. *Adv. Synth. Catal.* **2010**, *352*, 373–378. [CrossRef]
12. Zhou, Y.; Li, J.; Ji, X.; Zhou, W.; Zhang, X.; Qian, W.; Jiang, H.; Liu, H. Silver- and Gold-Mediated Domino Transformation: A Strategy for Synthesizing Benzo[e]indolo[1,2-*a*]pyrrolo/pyrido[2,1-*c*][1,4]diazepine-3,9-diones. *J. Org. Chem.* **2011**, *76*, 1239–1249. [CrossRef]
13. Feng, E.; Zhou, Y.; Zhao, F.; Chen, X.; Zhang, L.; Jiang, H.; Liu, H. Gold-catalyzed tandem reaction in water: An efficient and convenient syn-thesis of fused polycyclic indoles. *Green Chem.* **2012**, *14*, 1888–1895. [CrossRef]
14. Ji, X.; Zhou, Y.; Wang, L.; Zhao, L.; Jiang, H.; Liu, H. Au(I)/Ag(I)-catalyzed cascade approach for the synthesis of benzo[4,5]imidazo[1,2-*c*]pyrrolo[1,2-*a*]quinazolinones. *J. Org. Chem.* **2013**, *78*, 4312–4318. [CrossRef] [PubMed]
15. Qiao, J.; Jia, X.; Li, P.; Liu, X.; Zhao, J.; Zhou, Y.; Wang, J.; Liu, H.; Zhao, F. Gold-catalyzed Rapid Construction of Nitrogen-containing Heter-ocyclic Compound Library with Scaffold Diversity and Molecular Complexity. *Adv. Synth. Catal.* **2019**, *361*, 1419–1440. [CrossRef]
16. Jia, X.; Li, P.; Liu, X.; Lin, J.; Chu, Y.; Yu, J.; Wang, J.; Liu, H.; Zhao, F. Green and Facile Assembly of Diverse Fused N-Heterocycles Using Gold-Catalyzed Cascade Reactions in Water. *Molecules* **2019**, *24*, 988. [CrossRef]

17. Zhou, Y.; Zhai, Y.; Ji, X.; Liu, G.; Feng, E.; Ye, D.; Zhao, L.; Jiang, H.; Liu, H. Gold-Catalyzed One-Pot Cascade Construction of Highly Functionalized Pyrrolo[1,2-*a*]quinolin-1(2*H*)-ones. *J. Org. Chem.* **2009**, *74*, 7344–7348. [CrossRef]
18. Naidu, S.; Reddy, S.R. Copper-catalyzed tandem reaction in ionic liquid: An efficient reusable catalyst and solvent media for the synthesis of fused poly hetero cyclic compounds. *RSC Adv.* **2016**, *6*, 62742–62746. [CrossRef]
19. Naidu, S.; Reddy, S.R. A Green and Recyclable Copper and Ionic Liquid Catalytic System for the Construction of Polyheterocyclic Compounds via One-pot Tandem Coupling Reaction. *ChemistrySelect* **2017**, *2*, 1196–1201. [CrossRef]
20. Zheng, Y.; Liu, J.; Lei, X. Ru-Catalyzed cascade reaction of α,ω-alkynoic acids and arylethylamines towards the synthesis of aryl-fused hetero-cycles. *Org. Chem. Front.* **2020**, *7*, 660–665. [CrossRef]
21. Kshirsagar, U.A. Recent developments in the chemistry of quinazolinone alkaloids. *Org. Biomol. Chem.* **2015**, *13*, 9336–9352. [CrossRef] [PubMed]
22. Brožič, P.; Turk, S.; Adeniji, A.O.; Konc, J.; Janežič, D.; Penning, T.M.; Rižner, T.L.; Gobec, S. Selective Inhibitors of Aldo-Keto Reductases AKR1C1 and AKR1C3 Discovered by Virtual Screening of a Fragment Library. *J. Med. Chem.* **2012**, *55*, 7417–7424. [CrossRef]
23. Herrero, M.T.; Diaz de Sarralde, J.; SanMartin, R.; Bravo, L.; Dominguez, E. Cesium Carbonate-Promoted Hydroamidation of Alkynes: En-amides, Indoles and the Effect of Iron(III) Chloride. *Adv. Synth. Catal.* **2012**, *354*, 3054–3064. [CrossRef]
24. Conde, N.; SanMartin, R.; Herrero, M.T.; Domínguez, E. Palladium NNC Pincer Complex as an Efficient Catalyst for the Cycloisomerization of Alkynoic Acids. *Adv. Synth. Catal.* **2016**, *358*, 3283–3292. [CrossRef]
25. Sheldon, R.A. Fundamentals of green chemistry: Efficiency in reaction design. *Chem. Soc. Rev.* **2012**, *41*, 1437–1451. [CrossRef]
26. Jeon, S.J.; Li, H.; Walsh, P.J. A Green Chemistry Approach to a More Efficient Asymmetric Catalyst: Solvent-Free and Highly Concentrated Alkyl Additions to Ketones. *J. Am. Chem. Soc.* **2005**, *127*, 16416–16425. [CrossRef]
27. Mahmoud, M.A.; El-Sayed, M.A. Enhancing Catalytic Efficiency of Hollow Palladium Nanoparticles by Photothermal Heating of Gold Nano-particles Added to the Cavity: Palladium–Gold Nanorattles. *ChemCatChem* **2014**, *6*, 3540–3546. [CrossRef]
28. Nebra, N.; Monot, J.; Shaw, R.; Martin-Vaca, B.; Bourissou, D. 1,3-Bis(thiophosphinoyl)indene: A Unique and Versatile Scaffold for Original Polymetallic Complexes. *ACS Catal.* **2013**, *3*, 2930–2934. [CrossRef]
29. Lambert, C.; Utimoto, K.; Nozaki, H. Palladium(II) catalyzed cyclization of alkynoic acids. *Tetrahedron Lett.* **1984**, *25*, 5323–5326. [CrossRef]
30. Wakabayashi, T.; Ishii, Y.; Ishikawa, K.; Hidai, M. A Novel Catalyst with a Cuboidal PdMo3S4 Core for the Cyclization of Alkynoic Acids to Enol Lactones. *Angew. Chem. Int. Ed.* **1996**, *35*, 2123–2124. [CrossRef]
31. Cordi, A.; Spedding, M.; Serkiz, B.; Lepagnol, J.; Desos, P.; Morain, P. Preparation of (3aS)-5,5-Dioxo-2,3,3a,4-tetrahydro-1H-pyrrolo[2,1-c][1,2,4]benzothiadiazine AMPA Receptor Agonist. Europen Patent EP692484, 17 January 1996.
32. Gouliaev, A.H.; Larsen, M.; Varming, T.; Mathiesen, C.; Johansen, T.H.; Scheel-Krueger, J.; Olsen, G.M.; Nielsen, E.O. Preparation of Benzothiadiazines, Quinazolines, and Other Aryl-Fused Heterocycles as Positive AMPA-Receptor Modulators for Treatment of Memory and Learning Disorders. International Patent WO9942456, 26 August 1999.
33. Francotte, P.; de Tullio, P.; Podona, T.; Diouf, O.; Fraikin, P.; Lestage, P.; Danober, L.; Thomas, J.-Y.; Caignard, D.-H.; Pirotte, P. Synthesis and pharmacological evaluation of a second generation of pyridothiadiazine 1,1-dioxides acting as AMPA potentiators. *Bioorg. Med. Chem.* **2008**, *16*, 9948–9956. [CrossRef]
34. Carrozzo, M.M.; Battisti, U.M.; Cannazza, G.; Puia, G.; Ravazzini, F.; Falchicchio, A.; Perrone, S.; Citti, C.; Jozwiak, K.; Braghiroli, D.; et al. Design, stereoselective synthesis, configurational stability and biological activity of 7-chloro-9-(furan-3-yl)-2,3,3a,4-tetrahydro-1*H*-benzo[*e*]pyrrolo[2,1-*c*][1,2,4]thiadiazine 5,5-dioxide. *Bioorg. Med. Chem.* **2014**, *22*, 4667–4676. [CrossRef]
35. Battisti, U.M.; Citti, C.; Rastelli, G.; Pinzi, L.; Puja, G.; Ravazzini, F.; Ciccarella, G.; Braghirolia, D.; Cannazza, G. An unexpected reversal in the pharmacological stereoselectivity of benzothiadiazine AMPA positive allosteric modulators. *Med. Chem. Commun.* **2016**, *7*, 2410–2417. [CrossRef]
36. Destot-Wong, K.D.; Liang, K.; Gupta, S.K.; Favrais, G.; Schwendimann, L.; Pansiot, J.; Baud, O.; Spedding, M.; Lelièvre, V.; Mani, S.; et al. The AMPA receptor positive allosteric modulator, S18986, is neuroprotective against neonatal excitotoxic and inflammatory brain damage through BDNF synthesis. *Neuropharmacology* **2009**, *57*, 277–286. [CrossRef]
37. Yefimenko, N.; Portero-Tresserra, M.; Marti-Nicolovius, M.; Guillazo-Blanch, G.; Vale-Martinez, A. The AMPA receptor modulator S18986 in the prelimbic cortex enhances acquisition and retention of an odor-reward association. *Neurosci. Lett.* **2013**, *548*, 105–109. [CrossRef] [PubMed]
38. Malaquin, S.; Jida, M.; Courtin, J.; Laconde, G.; Willand, N.; Deprez, B.; Deprez-Poulain, R. Water-based conditions for the microscale parallel synthesis of bicyclic lactams. *Tetrahedron Lett.* **2013**, *54*, 562–567. [CrossRef]
39. De Sarro, A.; De Sarro, G.; Chimirri, A.; Grasso, S.; Monforte, A.-M.; Zappala, M. Anticonvulsant activity of pyrrolo[1′,2′:1,2]imidazo[4,5-b]pyridines, pyrrolo[2′,1′:2,3]imidazo[4,5-c]pyridines and pyrrolo[2,1-f]purines in DBA/2 mice. *Gen. Pharmacol.* **1994**, *25*, 1027–1031. [CrossRef]
40. Caccamese, S.; Principato, G.; Chimirri, A.; Grasso, S. Separation of the enantiomers of anticonvulsant tricyclic pyrroloimidazolones by enanti-oselective HPLC. A chiral recognition model and a chiroptical study. *Tetrahedron-Asymmetr.* **1996**, *7*, 2577–2584. [CrossRef]
41. Chimirri, A.; Grasso, S.; Monforte, P.; Zappalà, M.; Genchi, G. Pyrrolo[1′,2′:1,2]imidazo[4,5-b]pyridines, pyrrolo- [2′,1′:2,3]imidazo[4,5-c]pyridines and pyrrolo[2,1-f]purines as potential benzodiazepine ligands. *Farmaco* **1993**, *48*, 1261–1269. [CrossRef]

42. Bergbreiter, D.E.; Osburn, P.L.; Frels, J.D. Mechanistic Studies of SCS-Pd Complexes Used in Heck Catalysis. *Adv. Synth. Catal.* **2005**, *347*, 172–184. [CrossRef]
43. Gorunova, O.N.; Novitskiy, I.M.; Grishin, Y.K.; Gloriozov, I.; Roznyatovsky, V.A.; Khrustalev, V.N.; Kochetkov, K.A.; Dunina, V.V. When Applying the Mercury Poisoning Test to Palladacycle-Catalyzed Reactions, One Should Not Consider the Common Misconception of Mercury(0) Selectivity. *Organometallics* **2018**, *37*, 2842–2858. [CrossRef]
44. Yu, K.; Sommer, W.; Richardson, J.M.; Weck, M.; Jones, C.W. Evidence that SCS Pincer Pd(II) Complexes are only Precatalysts in Heck Catalysis and the Implications for Catalyst Recovery and Reuse. *Adv. Synth. Catal.* **2005**, *347*, 161–171. [CrossRef]
45. Widegren, J.A.; Finke, R.G. A review of the problem of distinguishing true homogeneous catalysis from soluble or other metal-particle hetero-geneous catalysis under reducing conditions. *J. Mol. Catal. A Chem.* **2003**, *198*, 317–341. [CrossRef]
46. Phan, N.T.S.; Van Der Sluys, M.; Jones, C.W. On the Nature of the Active Species in Palladium Catalyzed Mizoroki–Heck and Suzuki–Miyaura Couplings–Homogeneous or Heterogeneous Catalysis, A Critical Review. *Adv. Synth. Catal.* **2006**, *348*, 609–679. [CrossRef]
47. Schmidt, A.F.; Kurokhtina, A.A. Distinguishing Between the Homogeneous and Heterogeneous Mechanisms of Catalysis in the Mizoroki-Heck and Suzuki-Miyaura Reactions: Problems and Prospects. *Kinet. Catal.* **2013**, *53*, 714–730. [CrossRef]
48. CrysAlisPro, Agilent Technologies, Version 1.171.37.31 (Release 14 January 2014 CrysAlis171.NET) (Compiled 14 January 2014, 18:38:05). Available online: https://www.agilent.com/cs/library/usermanuals/Public/CrysAlis_Pro_User_Manual.pdf (accessed on 10 January 2022).
49. Dolomanov, O.V.; Bourhis, L.J.; Gildea, R.J.; Howard, J.A.K.; Puschmann, H. *OLEX2: A* complete structure solution, refinement and analysis program. *J. Appl. Cryst.* **2009**, *42*, 339–342. [CrossRef]
50. Sheldrick, G.M. A short history of *SHELX*. *Acta Crystallogr.* **2008**, *64*, 112–122. [CrossRef] [PubMed]
51. Macrae, C.F.; Bruno, I.J.; Chisholm, J.A.; Edgington, P.R.; McCabe, P.; Pidcock, E.; Rodriguez-Monge, L.; Taylor, R.; van de Streek, J.; Wood, P.A. Mercury CSD 2.0–New features for the visualization and investigation of crystal structures. *J. Appl. Cryst.* **2008**, *41*, 466–470. [CrossRef]
52. Spek, A.L. Single-crystal structure validation with the program *PLATON*. *J. Appl. Cryst.* **2003**, *36*, 7–13. [CrossRef]
53. Farrugia, L.J. WinGX suite for small-molecule single-crystal crystallography. *J. Appl. Cryst.* **1999**, *32*, 837–838. [CrossRef]
54. Aeberli, P.; Houlihan, W.J. Reaction of some oxo acids with anthranilic acid, anthranilamides, orthanilamides, and salicylamide. *J. Org. Chem.* **1968**, *33*, 2402–2407. [CrossRef]
55. Hadfield, J.A.; Pavlidis, V.H.; Roffey, J.R.A. Synthesis of Cytotoxic Pyrrolo[1,2-a]-benzimidazol-1-ones. *Synth. Commun.* **1995**, *25*, 1319–1329. [CrossRef]